Journal of
Cardiovascular Development and Disease

MDPI

Article

Pressure-Resolved Predicted Local Pulse Wave Velocity in the Human Abdominal Aorta: Association with Model-Derived Arterial Wall Mechanics

Jerker Karlsson [1,2,*], Jonas Stålhand [3], Carl-Johan Carlhäll [1,2] and Jan Engvall [1,2]

[1] Department of Health, Medicine, and Caring Sciences, Linköping University, 581 83 Linköping, Sweden
[2] Department of Clinical Physiology in Linköping, Region Östergötland, 581 85 Linköping, Sweden
[3] Solid Mechanics, Department of Management and Engineering, Linköping University, 581 83 Linköping, Sweden
* Correspondence: jerker.karlsson@liu.se

Abstract

Background: Pulse wave velocity (PWV) is commonly reported as a single value despite pressure-dependent arterial wall mechanics. We investigated whether associations between model-derived local PWV and constitutive parameters differed between diastolic and systolic loading. **Methods**: In this secondary analysis, previously collected abdominal aortic pressure and diameter measurements from 30 healthy participants were combined with a nonlinear constitutive model to identify c, k_1, and k_2. Local PWV was calculated from model-derived incremental stiffness using the Moens–Korteweg formulation. Multivariable regression and generalized estimating equations evaluated pressure-specific associations and interactions. **Results**: Model-derived local PWV was approximately 58% higher at systolic than at diastolic pressure. The pressure-by-$\log_{10}(k_2)$ interaction was statistically significant (B = −2.57; 95% CI, −3.88 to −1.25; false discovery rate [FDR]-adjusted $p < 0.001$). After FDR correction, k_1 and $\log_{10}(k_2)$ remained associated with local PWV at diastolic pressure, whereas only $\log_{10}(k_2)$ remained associated at systolic pressure. Sensitivity and robustness analyses supported the principal finding. **Conclusions**: Model-derived local PWV varied with arterial loading, and its relationship with the constitutive parameters differed between diastolic and systolic conditions. Within this modeling framework, local PWV should be interpreted in relation to the pressure at which it is evaluated. Evaluation against independent PWV measurements in larger, more diverse populations is warranted.

Keywords: abdominal aorta; arterial stiffness; constitutive modeling; pressure dependence; pulse wave velocity; vascular biomechanics

Academic Editors: Hua Zhang and De-Pei Li

Received: 15 August 2026
Revised: 25 October 2026
Accepted: 28 October 2026
Published: 3 November 2026

Copyright: © 2026 by the authors. Licensee MDPI, Basel, Switzerland. This article is an open access article distributed under the terms and conditions of the Creative Commons Attribution (CC BY) license.

1. Introduction

The aorta contributes to cardiovascular function by buffering the pulsatile output of the heart and maintaining peripheral perfusion. This Windkessel function depends on the mechanical properties of the arterial wall. Progressive stiffening of the large arteries is a characteristic of vascular aging and is associated with cardiovascular morbidity and mortality [1–3].

Pulse wave velocity (PWV) is widely used as a surrogate measure of arterial stiffness and can be assessed over arterial pathways of different lengths and anatomical composition. Carotid–femoral PWV (cfPWV) is the established regional measure of aortic stiffness and provides prognostic information based on pulse transit along the carotid–femoral pathway [4,5]. Global aortic pulse wave velocity (gPWV) has been proposed to characterize stiffness over a more extensive aortic pathway and has been investigated in relation to cardiovascular risk characteristics and cardiac function [6,7]. Brachial–ankle PWV (baPWV), which is widely used in Asia, includes contributions from both central elastic and peripheral muscular arteries [8]. Local pressure-resolved PWV differs from these transit-based measures by characterizing site-specific arterial behavior across a physiological pressure range. These measures interrogate different vascular segments and depend on different acquisition and computational assumptions; they should therefore be regarded as complementary rather than interchangeable.

Arterial wall mechanics are nonlinear and depend on loading conditions. As pressure increases during the cardiac cycle, the mechanical response of the arterial wall changes, resulting in a pressure-dependent increase in stiffness [9–11]. Consequently, PWV is not solely a fixed property of the arterial wall but also depends on the pressure at which it is evaluated. Measurements obtained under prevailing hemodynamic conditions may therefore provide limited information about local variations in wall mechanics across the physiological pressure range.

Biomechanical modeling provides an opportunity to examine local arterial mechanics across this pressure range. Constitutive models combined with inverse parameter estimation from in vivo pressure–radius data can characterize arterial wall properties and pressure-dependent stiffness [12–15]. Previous studies using the present cohort and modeling framework examined material parameters, wall stress, stiffness, and load-bearing behavior in the human abdominal aorta [16–19]. However, these studies did not investigate how the previously characterized wall mechanics are expressed as model-derived local PWV across the physiological pressure range. Pressure-dependent stiffness obtained within this framework can be incorporated into different PWV formulations, but it remains unclear how the resulting PWV estimates vary with pressure and computational method and whether their associations with the constitutive material parameters differ between loading conditions.

The aim of this secondary analysis was therefore to characterize pressure-resolved model-derived local PWV in the abdominal aorta and to compare estimates obtained using different computational formulations. We further examined whether associations between local PWV and the constitutive material parameters differed between diastolic and systolic loading conditions. We hypothesized that model-derived local PWV would vary across the physiological pressure range and between computational formulations and that its associations with the constitutive parameters would depend on loading condition.

2. Material and Methods

2.1. Ethics Approval and Informed Consent

The original study was approved by the Ethics Committee of Lund University, Sweden (Dnr LU457-90; 17 April 1991). All participants provided written informed consent in accordance with the Declaration of Helsinki.

2.2. Study Design and Participants

This study was a secondary analysis of previously collected pressure-diameter data from the infrarenal abdominal aorta. Thirty healthy volunteers were included: 15 men and 15 women aged 23–72 years. Recruitment was stratified by age and sex, with five men and

five women in each of three age groups: young (23–30 years), middle-aged (41–54 years), and elderly (67–72 years).

Participants reported being healthy, taking no regular medication, and having no history of cardiopulmonary, cerebrovascular, or peripheral vascular disease. None reported a family history of aortic aneurysmal disease, all were nonsmokers, and all had an ankle-brachial index of at least 1.0. None of the women used hormone replacement therapy [16].

All 30 participants from the original cohort had the required pressure-radius data and were included in the present secondary analysis; no participant-level dataset was excluded. The dataset has previously been used to investigate arterial wall material properties, stiffness components, wall stress, load-bearing behavior, and methodological performance [16–19]. The present analysis used the same measurements to address a distinct outcome: pressure-resolved model-derived local PWV. Comprehensive individual participant data are provided in Supplementary File S1 (S-File01).

2.3. Data Acquisition and Signal Processing

Simultaneous recordings of infrarenal abdominal aortic diameter and local intra-aortic pressure were obtained for each participant. Pulsatile diameter changes were measured noninvasively using ultrasound echo tracking, whereas intra-aortic pressure was recorded invasively using a catheter-based system. The measurement protocol, calibration procedures, and technical performance of the pressure and diameter recordings have been described previously [16,17]. The reported intraobserver coefficients of variation were 5% for static aortic diameter and 16% for pulsatile diameter change.

The pressure and radius signals were processed according to the previously established procedure [13]. Both signals were filtered using a zero-phase, fourth-order Butterworth low-pass filter with a cutoff frequency of 15 Hz and temporally aligned using an autoregressive model to correct for the offset between the measurement systems. For each participant, average pressure and radius cycles were calculated from 8–10 cardiac cycles. No individual cardiac cycle was excluded. The resulting average pressure-radius loop, which was used for parameter identification, is illustrated in Figure 1A.

2.4. Mechanical Modeling and Parameter Identification

Arterial wall mechanics were evaluated using the previously developed Pressure-Induced Material Parameter framework. Detailed descriptions of the constitutive equations, parameter-identification algorithm, and numerical validation have been published previously [12–15]. Briefly, the infrarenal abdominal aorta was represented as a homogeneous, incompressible, thin-walled cylindrical membrane. Equilibrium-based circumferential and axial stresses were calculated from the measured pressure-radius relationship and estimated wall geometry. The nonlinear mechanical response of the arterial wall was represented using a two-family Holzapfel-Gasser-Ogden strain-energy formulation.

The model included six subject-specific parameters: the isotropic material parameter c; the anisotropic material parameters k_1 and k_2; the mean fiber angle β; the unloaded radius $R0$; and the in situ axial stretch λ_z. The parameters were identified by minimizing the discrepancy between equilibrium-based and constitutively calculated circumferential and axial stresses over the averaged pressure-radius loop. The parameter-identification problem was solved using constrained nonlinear optimization. A schematic overview of the analysis workflow, including parameter identification and PWV estimation, is shown in Figure 2.

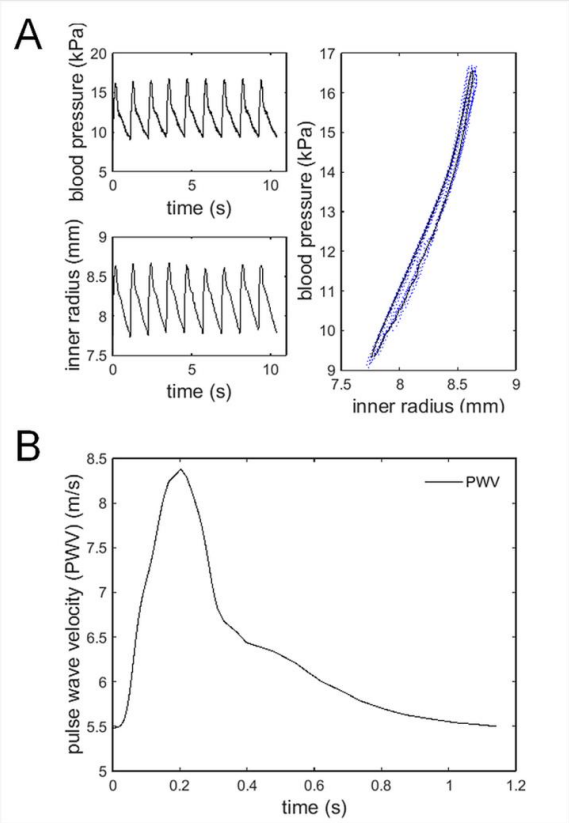


Figure 1. Illustration of signal computation. (**A**) From the acquired time-dependent pressure and radius data from cardiac cycles, an averaged pressure-radius loop can be formed. The average pressure-radius loop is utilized by the parameter identification process to produce the fitted stress-stretch-curve. The derivative of the stress-stretch-curve yields stiffness. (**B**) The stiffness is employed in the computation of a time-varying PWV that covers the cardiac cycle.

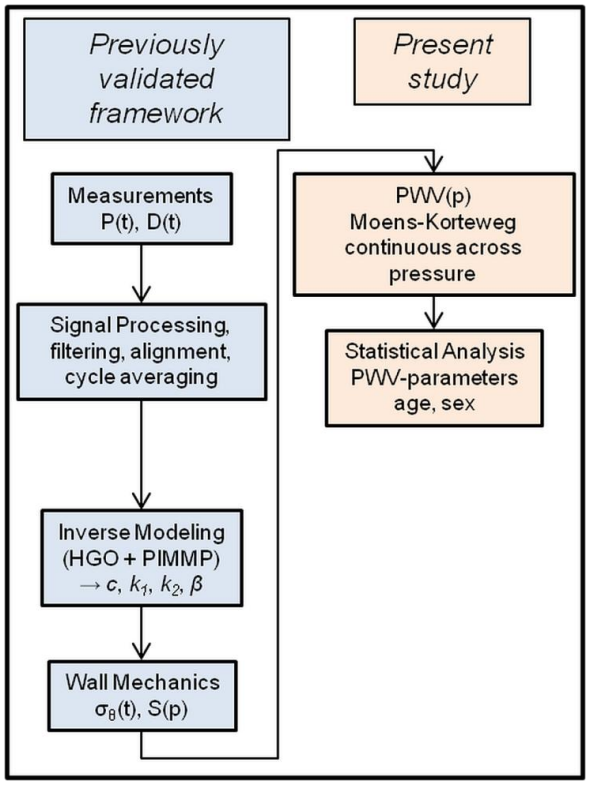


Figure 2. Conceptual workflow for pressure-resolved estimation of pulse wave velocity.

Data from in vivo measurements are processed and used in an established inverse modeling framework to obtain pressure-dependent arterial wall mechanics. The present study extends this framework by computing PWV as a continuous function of pressure and analyzing its association with model-derived wall-mechanical descriptors and relevant covariates. This workflow illustrates the distinction between the previously established wall-mechanical parameter identification and the new PWV-focused analysis performed in the present study.

2.5. Calculation of Pressure-Resolved Predicted Local PWV

Using the identified model parameters, circumferential wall stress was calculated as a function of pressure using Equation (4) in Table 1, and circumferential stiffness was defined as the incremental modulus according to Equation (3). Stiffness was evaluated continuously across the physiological pressure range and subsequently used to predict pressure-resolved local PWV in the infrarenal abdominal aorta. This predicted measure is hereafter referred to as model-derived local PWV.

As the primary method, model-derived local PWV was calculated using the Moens–Korteweg formulation given in Equation (8) in Table 1. Wall thickness was estimated from cross-sectional area relations as previously described [16]. This formulation allowed local PWV to be evaluated as a continuous function of pressure throughout the cardiac cycle. For each participant, PWV was extracted at diastolic blood pressure, systolic blood pressure, and intermediate pressure levels across the physiological pressure range. Model-derived local PWV at diastolic and systolic blood pressure was denoted PWV_{DBP} and PWV_{SBP}, respectively.

For comparison, PWV was also calculated using the Bramwell–Hill formulation given in Equation (11) in Table 1. Changes in aortic volume were derived from the measured diameter changes assuming cylindrical geometry. Estimated PWV based on age and blood pressure was calculated using the corresponding equation in Table 1. Throughout the manuscript, PWV_{MK} denotes model-derived local PWV calculated using the Moens–Korteweg formulation, PWV_{BH} denotes PWV calculated using the Bramwell–Hill formulation. ePWV denotes estimated PWV calculated from age and blood pressure according to Equation (10) in Table 1. A single equation was applied consistently across the cohort to provide a uniform age- and blood pressure-based comparator and to avoid introducing threshold-related discontinuities in age-dependent analyses. The complete calculation workflow is illustrated in Figure 2.

Table 1. Formulas used in the calculation of pulse wave velocity.

Eq.	Measure	Formula	Variables
1	Mean arterial pressure	$\mathrm{MAPauc} = \frac{1}{T} * \int_0^T P(t)dt$	P: blood pressure (Pa). t: time (s). T: duration of one cardiac cycle (s).
2	Distensibility coefficient, DC: the relative increase in arterial luminal area for a given increase in pressure *	$\mathrm{DC} = \frac{\Delta A}{\Delta P} * \frac{1}{A} = \frac{2D_d\Delta D + \Delta D^2}{\Delta P {D_d}^2}$	Circular luminal area assumed. The unit for DC is 10^{-3}/kPa. A: end diastolic lumen area (mm^2). ΔA: pulsatile lumen area (mm^2), calculated as $\Delta A = \pi(D_s^2 - D_d^2)/4$ where D_s and D_d are the internal diameters (mm) in systole and diastole, respectively. ΔP: local pulse pressure (kPa). ΔD: pulsatile diameter (mm). ΔD^2: squared pulsatile diameter (mm^2).
3	Incremental elastic modulus, E_{inc}: approximated by circumferential stiffness, $S_{\theta\theta}$ (marked by the superscript S)	$E^{\mathrm{S}}_{\mathrm{inc}} = \mathrm{S}_{\theta\theta} = \frac{\partial \sigma_\theta}{\partial \lambda_\theta}$	The unit for E_{inc} is kPa. The superscript S indicates circumferential stiffness, $S_{\theta\theta}$.

4	Circumferential stress, σ_θ	$\sigma_\theta = 2c\left[\lambda_\theta^2 - \frac{1}{(\lambda_\theta\lambda_z)^2}\right] + 4k_1(I-1) * e^{k_2(I_4-1)^2}\lambda_\theta^2 cos^2\beta$	c, k_1, k_2, β, λ_z: identified model parameters. I: invariant. λ_θ: circumferential stretch.
5	Peterson pressure-strain elastic modulus, E_P *	$E_P = \frac{P_s - P_d}{(D_s - D_d)/D_d}$	The unit for E_P is kPa. It represents the pressure change associated with an increase in relative luminal area. D_s and D_d are the systolic and diastolic diameters, while P_s and P_d are the systolic and diastolic blood pressures, respectively.
6	Static elastic modulus, E_{inc}^{P}, based on the Peterson pressure-strain elastic modulus (marked by the superscript P) *	$E_{inc}^{P} = \frac{2r}{h} * E_P$	h: wall thickness (m). r: radius (m). Both are measured in the vessel during diastole.
7	Time-independent elastic modulus (static), E_{inc}^{G}, was estimated from geometrical measurements (marked by the superscript G) *	$E_{inc}^{G} = 3 * \frac{1 + \frac{A_D}{WCSA}}{DC}$	A_D: end-diastolic luminal area (mm²). DC: distensibility coefficient. WCSA: wall cross-sectional area (mm²), calculated as WCSA $= \pi(D_e^2 - D_i^2)/4$, where D_e and D_i are the outer and inner diastolic diameters, respectively.
8	Pulse wave velocity according to the Moens–Korteweg equation, PWV_{MK}	$PWV_{MK} = \sqrt{\frac{E_{inc}h}{2r\rho}}$	PWV (m/s), ρ: blood density (1060 kg/m³), h: wall thickness, r: inner radius, E_{inc}: incremental elastic modulus. PWV_{MK} was used with different estimates of E_{inc}, producing a local aortic PWV for the abdominal aorta. Wall thickness h can be obtained from estimated arterial cross-sectional area A_{cr}, defined as $A_{cr} = 2\pi r_0 h$, according to formulas for the abdominal aorta in males and females from [16]: $A_{cr} = 19.60 + 0.80 * age$ (males) and $A_{cr} = 20.52 + 0.56 * age$ (females), with age is in years and A_{cr} in mm².
9	Mean pulse wave velocity, $mPWV_{MK}^{S}$	$mPWV_{MK}^{S} = \frac{1}{T} * \int_0^T PWV_{MK}^{S} dt$	T: duration of one cardiac cycle (s).
10	Estimated pulse wave velocity, ePWV	ePWV $= 4.62 - 0.13 * age + 0.0018 * age^2 + 0.0006 * age * MAP + 0.0284 * MAP$	age: age (years). MAP = 0.42 * PP+ DBP (mmHg), where PP is pulse pressure and DBP is diastolic blood pressure. ePWV was calculated from age and brachial blood pressure according to Greve et al. [20].
11	Pulse wave velocity according to the Bramwell–Hill equation, PWV_{BH}	$PWV_{BH} = \frac{1}{\sqrt{DC * \rho}}$	DC: distensibility coefficient. ρ: blood density (1060 kg/m³).

* Formulas taken from [3].

2.6. Statistical Analysis

Continuous variables are presented as mean ± standard deviation (SD). Distributions were assessed visually and using the Shapiro–Wilk test. Because k_2 was right-skewed ($p < 0.001$), $\log_{10}(k_2)$, which did not deviate significantly from normality ($p = 0.189$), was used in the primary regression analyses.

Age- and sex-group differences in pressure-resolved model-derived local PWV were evaluated using two-way analysis of variance, supplemented by general linear models, for the comparisons presented in Supplementary File S2 (S-File02), Table S2.1. Associations between the constitutive parameters and model-derived local PWV were assessed using Pearson correlations, with Spearman rank correlations used as a distribution-free sensitivity analysis.

Separate multivariable linear regression models were constructed for model-derived local PWV at diastolic pressure, PWV_{DBP}, and systolic pressure, PWV_{SBP}, with c, k_1, and $\log_{10}(k_2)$ entered simultaneously as explanatory variables. Unstandardized regression coefficients with 95% confidence intervals and p-values were reported, together with R^2 and

adjusted R^2. Variance inflation factors and tolerance were used to assess collinearity, and regression assumptions were evaluated using residual diagnostics.

Differences in parameter-PWV associations between diastolic and systolic loading conditions were tested using generalized estimating equations with robust standard errors, accounting for the two PWV observations within each participant. The model included pressure level, c, k_1, $\log_{10}(k_2)$, and the interaction between pressure level and each material parameter.

The pressure-dependent increase in PWV was defined as $\Delta PWV = PWV_{SBP} - PWV_{DBP}$ and analyzed using multivariable linear regression with c, k_1, and $\log_{10}(k_2)$ as explanatory variables.

Sensitivity analyses included comparison of models using k_2 and $\log_{10}(k_2)$ and assessment of the association between $\log_{10}(k_2)$ and PWV_{SBP} after adjustment for age and sex. Robustness of the PWV_{SBP} and ΔPWV models was assessed using nonparametric bootstrap resampling with 3000 iterations and leave-one-out analyses. Bootstrap-derived 95% confidence intervals were calculated for the regression coefficients, and potentially influential observations were evaluated using Cook's distance.

The Benjamini–Hochberg false discovery rate procedure was applied jointly to the following 12 tests: the three material-parameter coefficients in each of the PWV_{DBP}, PWV_{SBP}, and ΔPWV models and the three parameter-by-pressure interaction terms. Unadjusted and FDR-adjusted p-values are reported.

The regression analyses were exploratory. Because the constitutive parameters, pressure-dependent stiffness, and model-derived local PWV arose from the same pressure-radius data and modeling framework, associations were interpreted as descriptive relationships among internally related model outputs rather than as independent causal effects. All tests were two-sided, with $p < 0.05$ considered statistically significant.

2.7. Software

All signal processing, mechanical modeling, and PWV calculations were performed using MATLAB version 8.4 (R2014b;MathWorks, Natick, MA, USA). Statistical analyses were performed using IBM SPSS Statistics version 26 (IBM Corp., Armonk, NY, USA) and Python version 3.12.15. Python-based analyses used pandas version 2.2.2, NumPy version 1.26.4, SciPy version 1.13.1, statsmodels version 0.15.0, and scikit-learn version 1.5.1. Leave-one-out analyses and Benjamini–Hochberg false discovery rate corrections were performed in Python.

3. Results

3.1. Study Population and Model Parameters

All 30 participants, comprising 15 men and 15 women, were included in the present analysis; no participant was excluded. Participant characteristics are summarized in Table 2, and individual participant data are provided in S-File01. The six identified model parameters, c, k_1, k_2, β, $R0$, and λ_z, are presented in Table 3. No statistically significant differences in these parameters were observed between men and women.

Table 2. Characteristics of the study population.

	Age (Years)	Height * (cm)	Weight * (kg)	BMI * (kg/m²)	BSA * (m²)
Men					
Young (n = 5)	24.8 ± 1.9	177.4 ± 10.1	71.4 ± 8.6	22.6 ± 0.8	1.87 ± 0.17
Middle-aged (n = 5)	47.6 ± 5.0	180.0 ± 6.2 †	84.0 ± 9.5 †	25.9 ± 1.9†	2.05 ± 0.15 †
Elderly (n = 5)	69.6 ± 1.5	181.6 ± 5.3	87.2 ± 12.3	26.3 ± 2.5	2.09 ± 0.17
Women					
Young (n = 5)	25.4 ± 2.8	170.8 ± 7.1 ‡	59.0 ± 8.4‡	20.2 ± 1.7 ‡	1.67 ± 0.15 ‡

Middle-aged (n = 5)	49.2 ± 3.2	170.4 ± 5.0	67.0 ± 9.6	23.2 ± 4.2	1.78 ± 0.11
Elderly (n = 5)	68.8 ± 2.0	170.4 ± 8.0	64.6 ± 8.0	22.3 ± 3.1	1.75 ± 0.12

Data are presented as mean ± SD. Unless otherwise indicated, values are based on five participants per sex and age group. * Weight, height, body surface area, and body mass index were unavailable for two middle-aged men and one young woman; no missing values were imputed. † Based on three participants. ‡ Based on four participants. No formal statistical comparisons were performed. BMI, body mass index; BSA, body surface area. Modified from [17,18]. Licensed under CC BY 4.0 (https://creativecommons.org/licenses/by/4.0/, accessed on 13 March 2026).

Table 3. Model parameters.

Model Parameters	Male	Female
c (kPa)	131.50 ± 90.00	101.65 ± 63.75
k_1 (kPa)	14.18 ± 20.94	8.64 ± 10.00
k_2 (-)	196.76 ± 264.22	134.95 ± 175.15
β (°)	42.38 ± 4.38	42.31 ± 3.82
$R0$ (mm)	7.80 ± 1.78	6.77 ± 1.23
λ_z (-)	1.03 ± 0.02	1.03 ± 0.02

Data are mean ± SD. No statistically significant differences were observed between men and women for any of the six model parameters [17,18]. Licensed under CC BY 4.0 (https://creativecommons.org/licenses/by/4.0/, accessed on 13 March 2026).

3.2. Effects of Pressure Level and Computational Formulation

PWV estimates differed according to pressure level and computational formulation (Figure 3). Model-derived local PWV calculated using the Moens–Korteweg formulation was approximately 58% higher at systolic than at diastolic pressure. PWV_{MK} at systolic pressure was significantly higher than PWV_{MK} at diastolic pressure, whereas PWV_{MK} at diastolic pressure was numerically similar to PWV_{BH} and ePWV. Detailed comparisons are provided in S-File02.

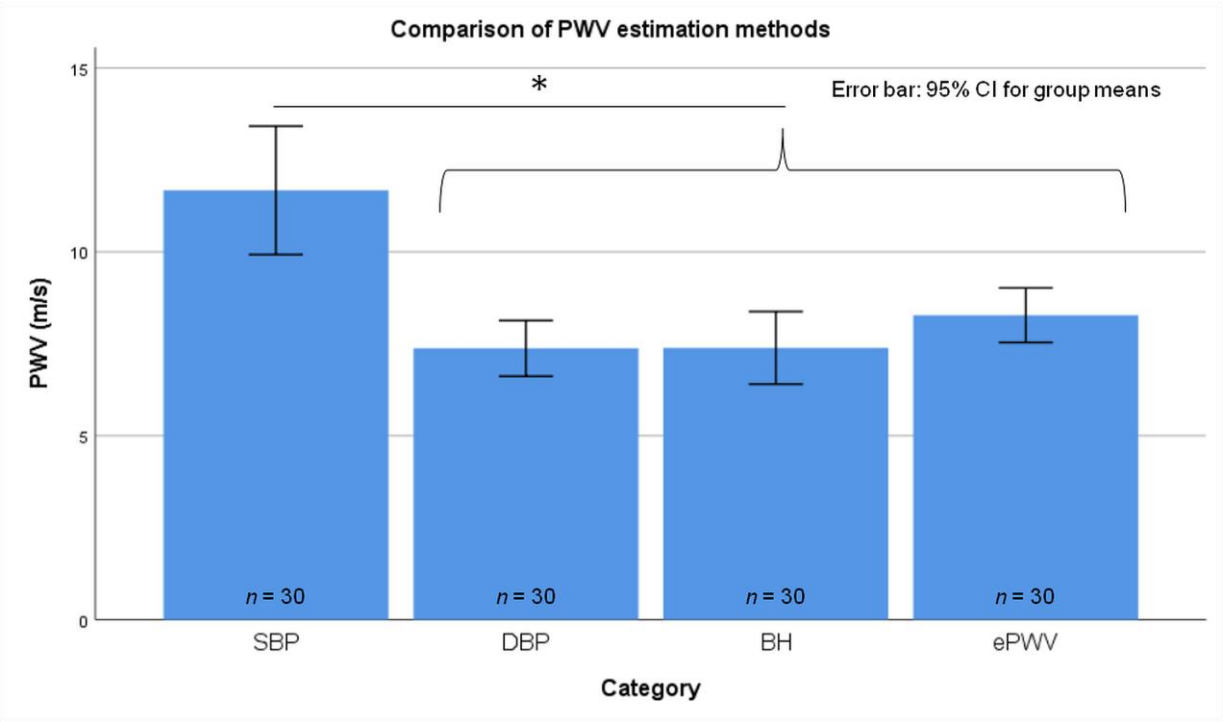


Figure 3. Comparison of pulse wave velocity estimates obtained using different computational formulations and pressure levels. Model-derived local PWV calculated using the Moens–Korteweg

formulation (PWV_{MK}) at diastolic blood pressure (DBP) and systolic blood pressure (SBP) is compared with PWV calculated using the Bramwell–Hill formulation (PWV_{BH}) and estimated PWV (ePWV). Bars represent group means, and error bars indicate 95% confidence intervals. PWV_{MK} at SBP was significantly higher than PWV_{MK} at DBP (* $p < 0.05$), whereas PWV_{MK} at DBP yielded values similar to PWV_{BH} and ePWV at the group level. Detailed comparisons are provided in Supplementary file S2 (S-File02).

3.3. Pressure Dependence Across Age and Sex Groups

Model-derived local PWV increased with pressure in both sexes and across all three age groups (Figure 4). At diastolic pressure, PWV ranged from approximately 5.1 m/s in young men to 10.0 m/s in elderly men and from 5.6 m/s in young women to 8.8 m/s in elderly women. Absolute PWV values showed an age-related pattern, with significant differences between the young and elderly groups as indicated in Figure 4 and Supplementary File S2 (S-File02).

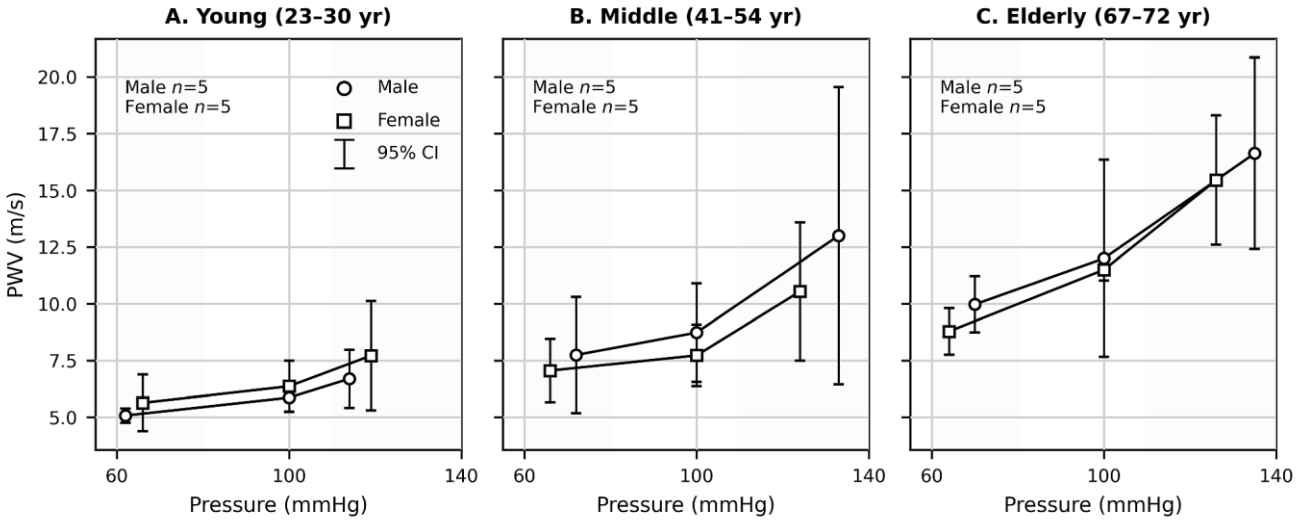


Figure 4. Pressure dependence of model-derived local pulse wave velocity in men and women across age groups. Model-derived local PWV calculated using the Moens–Korteweg formulation is shown at group mean diastolic blood pressure, 100 mmHg, and group mean systolic blood pressure for young, middle-aged, and elderly participants. Circles denote men and squares denote women; values are means with 95% confidence intervals ($n = 5$ per sex and age group). Lines connect pressure levels for visual guidance. Superscripts a and b indicate $p < 0.05$ for young versus elderly participants among men and women, respectively. Gray areas indicate the diastolic and systolic blood pressure ranges. Group comparisons are provided in Supplementary File S2 (S-File02).

3.4. Correlation Analyses

The strongest correlations with model-derived local PWV were observed for c at diastolic pressure and for $\log_{10}(k_2)$ at systolic pressure. The isotropic parameter c was strongly correlated with PWV_{DBP} (r = 0.900), whereas $\log_{10}(k_2)$ showed the strongest correlation with PWV_{SBP} (r = 0.921). The pressure-dependent increase in PWV was also strongly correlated with $\log_{10}(k_2)$ (r = 0.863). Corresponding Spearman rank correlations are provided in Supplementary File S4 (S-File04, Table S4.4).

3.5. Associations Between Material Parameters and Model-Derived Local PWV

In the multivariable model for PWV_{DBP}, c, k_1, and $\log_{10}(k_2)$ were statistically associated with the outcome before correction for multiple testing (Table 4). After FDR correction, the associations remained statistically significant for k_1 and $\log_{10}(k_2)$, but not for c (FDR-adjusted $p = 0.065$). The model had $R^2 = 0.933$ and adjusted $R^2 = 0.925$.

Table 4. Exploratory associations between pressure-resolved model-derived local PWV and constitutive material parameters.

Analysis	Term	*B*	95% CI	*p*	FDR-Adjusted *p*	R^2	Adjusted R^2
PWV_{DBP}	c	0.007	0.001 to 0.013	0.033	0.065	0.933	0.925
	k_1	0.042	0.026 to 0.058	<0.001	<0.001		
	$\log_{10}(k_2)$	2.167	1.493 to 2.841	<0.001	<0.001		
PWV_{SBP}	C	0.013	−0.007 to 0.032	0.190	0.285	0.870	0.855
	k_1	0.023	−0.028 to 0.073	0.371	0.407		
	$\log_{10}(k_2)$	4.736	2.576 to 6.895	<0.001	<0.001		
GEE interactions	c × pressure level	−0.006	−0.017 to 0.005	0.296	0.395		
	k_1 × pressure level	0.019	−0.004 to 0.042	0.103	0.177		
	$\log_{10}(k_2)$ × pressure level	−2.569	−3.884 to −1.253	<0.001	<0.001		
ΔPWV	c	0.006	−0.010 to 0.023	0.460	0.460	0.754	0.725
	k_1	−0.019	−0.063 to 0.024	0.373	0.407		
	$\log_{10}(k_2)$	2.569	0.723 to 4.414	0.008	0.020		

B, unstandardized regression coefficient; CI, confidence interval; FDR, false discovery rate; GEE, generalized estimating equation; PWV, pulse wave velocity. c and k_1 are expressed in kPa. Systolic pressure was the reference level in the GEE model; the interaction coefficients therefore represent the difference in slope at diastolic relative to systolic pressure. The Benjamini–Hochberg procedure was applied jointly to the 12 material-parameter and interaction tests. R^2 and adjusted R^2 are reported for the ordinary least-squares models only. Coefficients describe associations within the shared modeling framework and should not be interpreted as independent mechanistic effects.

In the model for PWV_{SBP}, $\log_{10}(k_2)$ was statistically associated with the outcome ($B = 4.736$; 95% CI, 2.576–6.895; $p < 0.001$; FDR-adjusted $p < 0.001$), whereas c and k_1 were not. The model had $R^2 = 0.870$ and adjusted $R^2 = 0.855$ (Table 4). The complete multiplicity-adjusted results are provided in Supplementary File S3 (S-File03).

The generalized estimating equation analysis showed a statistically significant interaction between pressure level and $\log_{10}(k_2)$ ($B = -2.57$; 95% CI, −3.88 to −1.25; $p < 0.001$; FDR-adjusted $p < 0.001$), indicating that the association between $\log_{10}(k_2)$ and model-derived local PWV differed between diastolic and systolic loading conditions. The corresponding pressure-by-parameter interactions were not statistically significant for c ($p = 0.296$; FDR-adjusted $p = 0.395$) or k_1 ($p = 0.103$; FDR-adjusted $p = 0.177$) (Table 4).

3.6. Pressure-Dependent Increase in PWV

The pressure-dependent increase in model-derived local PWV, ΔPWV, was 4.30 ± 2.90 m/s. In the multivariable model, $\log_{10}(k_2)$ was statistically associated with ΔPWV ($B = 2.57$; 95% CI, 0.72–4.41; $p = 0.008$; FDR-adjusted $p = 0.020$), whereas c ($p = 0.460$) and k_1 ($p = 0.373$) were not. The model had $R^2 = 0.754$ and adjusted $R^2 = 0.725$ (Table 4).

3.7. Sensitivity and Robustness Analyses

Adjustment for age and sex did not materially alter the principal PWV_{SBP} result. In the adjusted model, $\log_{10}(k_2)$ remained statistically associated with PWV_{SBP} ($B = 3.59$; 95% CI, 0.98–6.20; $p = 0.009$), whereas age ($p = 0.075$) and sex ($p = 0.592$) were not statistically significant. Detailed sensitivity and diagnostic results are provided in Supplementary File S3 (S-File03).

Bootstrap-derived 95% confidence intervals for $\log_{10}(k_2)$ excluded zero in both the PWV_{SBP} model (2.68–7.13) and the ΔPWV model (1.00–4.35). The associations remained statistically significant in all 30 leave-one-out iterations for both outcomes. Cook's distance identified potentially influential observations, but omission of any single participant did not remove the statistical significance of the associations. Detailed robustness results are provided in Supplementary File S4 (S-File04).

4. Discussion

4.1. Principal Findings

Model-derived local PWV was pressure-dependent, with higher values at systolic than at diastolic pressure. The principal finding was that its relationship with the constitutive material parameters varied with arterial loading conditions. In particular, the stronger association with $\log_{10}(k_2)$ at systolic pressure and the corresponding pressure-by-parameter interaction indicate a pressure-specific relationship between local PWV and arterial wall mechanics. Within the present modeling framework, local PWV should therefore be interpreted in relation to the pressure at which it is evaluated, rather than as a pressure-independent measure of arterial wall behavior.

4.2. Pressure Dependence and PWV Estimation Approaches

The pressure dependence of model-derived local PWV is consistent with the nonlinear mechanical behavior of the arterial wall [2,3,10]. As pressure increases, the wall is evaluated at a higher point on its nonlinear stress–strain relationship, where incremental stiffness is greater [2,10]. Variation in local PWV over the cardiac cycle therefore reflects the response of the same arterial wall under different loading conditions rather than a change in its material constitution. This distinction is important when PWV estimates obtained at different pressures are compared or interpreted as measures of arterial stiffness [2,3]. More broadly, PWV may reflect dynamic changes in local vascular homeostasis and the interaction between arterial properties and systemic physiological conditions, rather than arterial wall stiffness alone [21].

Consistent with the pressure dependence of PWV_{MK}, estimates at systolic pressure were higher than those at diastolic pressure. PWV_{MK} at diastolic pressure yielded estimates that were similar to PWV_{BH} and ePWV at the group level. However, these observations should not be interpreted as evidence of interchangeability between methods. PWV_{MK} was derived from model-based incremental stiffness at a specified pressure [2,3], PWV_{BH} from the measured pressure–diameter relationship [4], and ePWV from age and blood pressure. Single-value estimates may therefore not capture the full pressure-dependent variation in PWV_{MK}. Without an independently measured local PWV reference, the present data do not permit conclusions regarding validation between these approaches.

4.3. Pressure-Specific Associations with Material Parameters

The association between model-derived local PWV and $\log_{10}(k_2)$ is consistent with the nonlinear and anisotropic behavior represented by the constitutive model [10,16]. In this formulation, k_2 governs the exponential increase in the fiber-related contribution to wall stress with increasing deformation [10]. The significant pressure-by-$\log_{10}(k_2)$ interaction indicates that this association varied with loading. The stronger association at systolic pressure may reflect an increasing influence of anisotropic wall mechanics, consistent with observations that collagen-related contributions to aortic wall stiffness become more prominent as pressure and distension increase [9,16]. However, because $\log_{10}(k_2)$ is a

model parameter rather than a direct measure of collagen behavior, this interpretation does not establish a specific microstructural mechanism.

At diastolic pressure, local PWV was associated with a broader combination of constitutive parameters. After FDR correction, the associations with k_1 and $\log_{10}(k_2)$, but not with c, remained statistically significant. This may indicate that PWV at lower loading is related to several aspects of the constitutive response, whereas the systolic association pattern was more specific to $\log_{10}(k_2)$. Joint parameter identification and collinearity between c and $\log_{10}(k_2)$, however, limit their statistical and mechanistic separation.

5. Methodological Considerations

The interaction analysis compared parameter associations between diastolic and systolic loading within the same participants. The significant pressure-by-$\log_{10}(k_2)$ interaction therefore indicates a systematic change in the association across loading conditions. This contrast should be interpreted within the shared mathematical framework from which the constitutive parameters, wall stiffness, and model-derived local PWV were derived. The interaction remained significant after correction for multiple testing. In separate complementary analyses, the association between $\log_{10}(k_2)$ and PWV_{SBP} remained significant after adjustment for age and sex, while rank-based analyses supported the associations of $\log_{10}(k_2)$ with both PWV_{SBP} and ΔPWV. Because the $\log_{10}(k_2)$ coefficient in the ΔPWV model reflects the corresponding difference between systolic and diastolic associations, bootstrap and leave-one-out analyses of the ΔPWV model provided complementary information on the stability of this contrast.

The thin-walled membrane model neglects transmural stress gradients. Although this may affect absolute stress distributions, previous work indicates that key functional outputs, including stiffness and load-bearing behavior, are adequately captured under physiological conditions [19]. From a methodological perspective, reporting model-derived local PWV at a defined pressure, or across a physiological pressure range, may be more informative than reporting a single value without an explicit pressure reference.

Established regional and global PWV measures currently have greater clinical relevance than the present model-derived local approach. However, they characterize pulse-wave propagation over longer vascular pathways and do not provide the same pressure-resolved information about local abdominal aortic wall behavior. The present approach should therefore be regarded as complementary rather than interchangeable with regional cfPWV or gPWV. Whether pressure-resolved local PWV provides incremental physiological or clinical information requires direct comparison with these established measurements [3,6–8].

6. Limitations

The small sample of healthy participants limits precision and generalizability, particularly to individuals with cardiovascular disease, while the historical data limit their use as contemporary reference values. The analysis was restricted to the abdominal aorta, and local abdominal aortic PWV is not interchangeable with regional carotid–femoral PWV. Uncertainty in ultrasound-derived diameter measurements may propagate to derived stiffness and local PWV, although synchronized pressure recording, signal alignment, filtering, and cycle averaging reduced random variability. Interobserver and repeat-acquisition reproducibility data were unavailable from the original study and therefore could not be assessed in this secondary analysis. The model does not account for active smooth muscle tone or viscoelasticity, and absolute PWV estimates may depend on arterial geometry, estimated wall thickness, the constitutive model, and the PWV formulation. Arterial wall thickness was not measured directly but estimated from age- and sex-specific

relationships, which may have influenced the estimated material parameters and pressure-resolved PWV values.

The constitutive parameters, wall stiffness, and model-derived local PWV were derived from the same pressure–radius data and are mathematically coupled; hence, high correlations and coefficients of determination do not represent independent predictive performance. Collinearity between c and $\log_{10}(k_2)$ further limits separation of their associations. Cook's distance identified potentially influential observations. Although leave-one-out analyses supported internal stability, external validation against an independently measured local PWV reference was not performed. These considerations limit mechanistic inference and generalizability.

7. Conclusions

Model-derived local PWV was pressure-dependent, and its association with the constitutive parameters differed between diastolic and systolic loading. The pressure-specific association with $\log_{10}(k_2)$ indicates that the relationship between local PWV and the modeled constitutive response varies with arterial loading. Within the present modeling framework, local PWV should therefore be interpreted and reported with explicit reference to the pressure at which it is evaluated. Further studies should assess reproducibility and evaluate pressure-resolved local PWV against independent measurements in larger, more diverse populations.

Supplementary Materials: The following supporting information can be downloaded at: https://www.mdpi.com/article/10.3390/jcdd13110567/s1; Supplementary File S1 (S-File01): Table S1.1 Individual Participant Characteristics, Blood Pressure, and Aortic Diameter Data; Supplementary File S2 (S-File02): Table S2.1. Pulse wave velocity estimates by sex, age group, pressure level, and calculation method; Supplementary File S3 (S-File03): Table S3.1. Collinearity diagnostics; Table S3.2. Sensitivity analysis of the association between log10(k2) and PWVSBP, adjusted for age and sex; Table S3.3. Benjamini–Hochberg false discovery rate (FDR) correction across the 12 tests; Supplementary File S4 (S-File04): Table S4.1. Bootstrap Results; Table S4.2. Leave-One-Out Analyses; Table S4.3. Cook's Distance Diagnostics; Table S4.4. Spearman Rank Correlations.

Author Contributions: J.K. and J.S. jointly developed the study concept and overall design. J.K. carried out all model computations as well as the statistical analyses. The interpretation of the results was undertaken collaboratively by J.K., J.S. and J.E. J.K. prepared the initial manuscript draft, while J.S., C.-J.C., and J.E. provided detailed critical revisions and feedback across multiple subsequent versions. All authors have read and agreed to the published version of the manuscript.

Funding: This research received financial support from Region Östergötland, the Medical Faculty at Linköping University (grant RÖ-977160), the Swedish Research Council (Grant 12661), and the Swedish Heart-Lung Foundation. These funding bodies provided salary support for J.K., but they had no involvement whatsoever in the study's design, data acquisition, analysis, interpretation, or in the preparation of the manuscript.

Informed Consent Statement: All participants provided written informed consent in accordance with the Declaration of Helsinki.

Institutional Review Board Statement: The original study was approved by the Ethics Committee of Lund University, Sweden (Dnr LU457-90; 17 April 1991).

Data Availability Statement: The data presented in this study are available on request from the corresponding author. Because the source measurements were acquired as part of an earlier

physiological protocol, data sharing may be subject to ethical and institutional restrictions applicable to the original material.

Acknowledgments: The authors wish to express their profound appreciation for the guidance, teaching, and enduring support of the late Toste Länne. As a trailblazer in interdisciplinary vascular physiology and surgery, his visionary leadership at Linköping University Hospital laid the foundation for this work, including the conception and recruitment of the study cohort on which this research is based.

Conflicts of Interest: The authors declare that they have no conflict of interest.

References

1. Sonesson, B.; Hansen, F.; Stale, H.; Länne, T. Compliance and diameter in the human abdominal aorta—The influence of age and sex. *Eur. J. Vasc. Surg.* **1993**, *7*, 690–697. https://doi.org/10.1016/s0950-821x(05)80718-2.
2. Nichols, W.W.; O'Rourke, M.F. *McDonald's Blood Flow in Arteries: Theoretical, Experimental and Clinical Principles*, 5th ed.; Hodder Arnold: London, UK, 2005.
3. Laurent, S.; Cockcroft, J.; Van Bortel, L.; Boutouyrie, P.; Giannattasio, C.; Hayoz, D.; Pannier, B.; Vlachopoulos, C.; Wilkinson, I.; Struijker-Boudier, H.; et al. Expert consensus document on arterial stiffness: Methodological issues and clinical applications. *Eur. Heart J.* **2006**, *27*, 2588–2605. https://doi.org/10.1093/eurheartj/ehl254.
4. Bramwell, J.C.; Hill, A.V. The velocity of pulse wave in man. *Proc. R. Soc. London. Ser. B Contain. Pap. A Biol. Character* **1922**, *93*, 298–306. https://doi.org/10.1098/rspb.1922.0022.
5. Peterson, L.H.; Jensen, R.E.; Parnell, J. Mechanical Properties of Arteries in Vivo. *Circ. Res.* **1960**, *8*, 622–639. https://doi.org/10.1161/01.RES.8.3.622.
6. Palmiero, P.; Maiello, M.; Daly, D.D.; Zito, A.; Ciccone, M.M.; Nanda, N.C. Relationship between global pulse wave velocity and diastolic dysfunction in postmenopausal women. *Int. J. Clin. Exp. Med.* **2014**, *7*, 5629–5635.
7. Lindenberger, M.; Ziegler, M.; Bjarnegård, N.; Ebbers, T.; Dyverfeldt, P. Regional and Global Aortic Pulse Wave Velocity in Patients with Abdominal Aortic Aneurysm. *Eur. J. Vasc. Endovasc. Surg.* **2024**, *67*, 506–513. https://doi.org/10.1016/j.ejvs.2023.09.040.
8. Park, J.B.; Sharman, J.E.; Li, Y.; Munakata, M.; Shirai, K.; Chen, C.H.; Jae, S.Y.; Tomiyama, H.; Kosuge, H.; Bruno, R.M.; et al. Expert Consensus on the Clinical Use of Pulse Wave Velocity in Asia. *Pulse* **2022**, *10*, 1–18. https://doi.org/10.1159/000528208.
9. Armentano, R.L.; Levenson, J.; Barra, J.G.; Fischer, E.I.; Breitbart, G.J.; Pichel, R.H.; Simon, A. Assessment of elastin and collagen contribution to aortic elasticity in conscious dogs. *Am. J. Physiol.-Heart Circ. Physiol.* **1991**, *260*, H1870–H1877. https://doi.org/10.1152/ajpheart.1991.260.6.H1870.
10. Holzapfel, G.A.; Gasser, T.C.; Ogden, R.W. A New Constitutive Framework for Arterial Wall Mechanics and a Comparative Study of Material Models. *J. Elast.* **2000**, *61*, 1–48. https://doi.org/10.1023/a:1010835316564.
11. Marsh, J.N.; Takiuchi, S.; Lin, S.J.; Lanza, G.M.; Wickline, S.A. Ultrasonic delineation of aortic microstructure: The relative contribution of elastin and collagen to aortic elasticity. *J. Acoust. Soc. Am.* **2004**, *115*, 2032–2040. https://doi.org/10.1121/1.1698887.
12. Schulze-Bauer, C.A.; Holzapfel, G.A. Determination of constitutive equations for human arteries from clinical data. *J. Biomech.* **2003**, *36*, 165–169. https://doi.org/10.1016/S0021-9290(02)00367-6.
13. Stålhand, J. Determination of human arterial wall parameters from clinical data. *Biomech. Model. Mechanobiol.* **2009**, *8*, 141–148. https://doi.org/10.1007/s10237-008-0124-3.
14. Smoljkić, M.; Vander Sloten, J.; Segers, P.; Famaey, N. Non-invasive, energy-based assessment of patient-specific material properties of arterial tissue. *Biomech. Model. Mechanobiol.* **2015**, *14*, 1045–1056. https://doi.org/10.1007/s10237-015-0653-5.
15. Gade, J.L.; Stålhand, J.; Thore, C.J. An in vivo parameter identification method for arteries: Numerical validation for the human abdominal aorta. *Comput. Methods Biomech. Biomed. Engin* **2019**, *22*, 426–441. https://doi.org/10.1080/10255842.2018.1561878.
16. Åstrand, H.; Stålhand, J.; Karlsson, J.; Karlsson, M.; Sonesson, B.; Länne, T. In vivo estimation of the contribution of elastin and collagen to the mechanical properties in the human abdominal aorta: Effect of age and sex. *J. Appl. Physiol.* **2011**, *110*, 176–187. https://doi.org/10.1152/japplphysiol.00579.2010.
17. Karlsson, J.; Stålhand, J.; Carlhäll, C.-J.; Länne, T.; Engvall, J. Abdominal Aortic Wall Cross-coupled Stiffness Could Potentially Contribute to Aortic Length Remodeling. *Artery Res.* **2022**, *28*, 113–127. https://doi.org/10.1007/s44200-022-00022-0.

18. Karlsson, J.; Stålhand, J.; Carlhäll, C.J.; Länne, T.; Engvall, J. An in vivo study of isotropic and anisotropic wall stress in a hyperelastic holzapfel-gasser-ogden model in the human abdominal aorta: Effects of age and sex. *Front. Physiol.* **2023**, *14*, 1128131. https://doi.org/10.3389/fphys.2023.1128131.
19. Karlsson, J.; Gade, J.-L.; Thore, C.-J.; Carlhäll, C.-J.; Engvall, J.; Stålhand, J. Evaluating the Stress State and the Load-Bearing Fraction as Predicted by an In Vivo Parameter Identification Method for the Abdominal Aorta. *Med. Sci.* **2025**, *13*, 9. https://doi.org/10.3390/medsci13010009.
20. Greve, S.V.; Blicher, M.K.; Kruger, R.; Sehestedt, T.; Gram-Kampmann, E.; Rasmussen, S.; Vishram, J.K.K.; Boutouyrie, P.; Laurent, S.; Olsen, M.H. Estimated carotid–femoral pulse wave velocity has similar predictive value as measured carotid–femoral pulse wave velocity. *J. Hypertens.* **2016**, *34*, 1279–1289. https://doi.org/10.1097/hjh.0000000000000935.
21. Yuen, C.; Devlin, A.M.; Bernatchez, P. Exploring pulse wave velocity as a vascular hemodynamic stress marker: More than just arterial stiffening? *Am. J. Physiol.-Heart Circ. Physiol.* **2026**, *330*, H243-H252. https://doi.org/10.1152/ajpheart.00638.2025.

Disclaimer/Publisher's Note: The statements, opinions and data contained in all publications are solely those of the individual author(s) and contributor(s) and not of MDPI and/or the editor(s). MDPI and/or the editor(s) disclaim responsibility for any injury to people or property resulting from any ideas, methods, instructions or products referred to in the content.